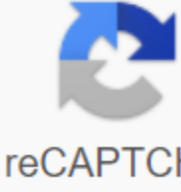


I'm not robot  reCAPTCHA

Continue

Polymer electrolyte membrane fuel cells (PEMFCs) have attracted a lot of attention over the past two decades as valuable alternative energy producers due to their high efficiency and low or zero pollutant emissions. In the present work, two gas diffusion electrodes (GDEs) for PEMFCs were produced with an ink containing carbon-containing platinum in the catalytic phase and sprayed on a carbon cloth substrate. Two aerograph nozzles of different sizes were used. The prepared GDEs were assembled into a fuel cell laboratory prototype with commercial electrolyte and bipolar plates and tested alternately as anode and cathode. Polarization measurements and electrochemical impedance spectroscopy (EIS) were carried out on the current, hydrogen-powered PEMFC from the idle voltage to the high current density. Experimental impedance spectra were equipped with an equivalent circuit model using the ZView software, which enabled the obtaining of critical parameters for the evaluation of fuel cell performance, such as ohmic resistance, charge transfer, and mass transmission resistance, the trends of which were investigated depending on the current density applied.

1. Introduction Polymer electrolyte membrane fuel cells (PEMFCs) are interesting alternative energy generators due to their high power density and conversion efficiency associated with modularity, low working temperature (less than 100°C) and environmentally friendly emission. However, commercial distribution of PEMFCs is still prevented by cost-cutting, electrocatalyst activity, and material resistance and stability [1-4]. The catalytic layer is the place where the redox reactions occur; therefore, its structural and wetted properties are of the utmost importance for the optimal operation of the fuel cell [5]. PEMFCs are usually catalyzed platinum, and the cost of the catalyst therefore has a major impact on the cost of these fuel cells. A massive use of FCs in the automotive industry therefore requires the search for a material alternative to a platinum catalyst. Much effort has been made in this area [6, 7], but Pt-based catalysts are still the most modern materials [3, 8, 9]. When designing an active catalyst, the Pt dispersion [10] must be taken into account in addition to the Pt load in order to maximize the active surface. In addition, ionomer content and distribution, microstructure and porosity are essential factors for providing a rapid proton transfer rate from the anode to the cathode. Of course, this must be achieved without increasing mass transmission resistance in order to achieve high efficiency in electrochemical conversion. In a PEMFC, you can Catalyst layer can be applied directly to the electrolytic membrane (catalyst-coated membrane (CCM)) or alternatively to the gas diffusion medium (GDM) [11, 12]. In the latter case, the so-called gas diffusion electrode (GDE) is obtained, which is a multilayered structure with a rather complex composition. For the preparation of a GDE, the catalyst powder (i.e. Pt Pt (c)) is coated on a gas diffusion medium (GDM). GDM usually consists of a sheet of macroporous carbon cloth or paper (usually referred to as a gas diffusion layer (GDL)) coated with a thin layer of soot and polytetrafluoroethylene, the so-called microporous layer (MPL). In the most recent literature, interest in the preparation of GDEs is increasing [13-18]. Catalytic layers are usually deposited with a variety of techniques such as brush pressure [19], ultrasonic syringes [13] and flexography printing [14] with an ink on the GDM, which is produced by dispersing the Pt/C catalyst in a solvent mixture. In the production of catalytic ink, many variables must be taken into account, such as the tenderness and ratio of the components or mixing and mixing time. All these factors help to define the appropriate rheological behaviour and stability of the ink [20] for the specific deposition technique. The performance of fuel cells and the influence of different components on them are usually assessed by polarization curves, which are useful for knowing the trend of cell potential and output power density depending on the current density. Therefore, such curves refer to the macroscopic behavior of the entire device and do not give accurate information about the effect of internal components. To solve this problem, electrochemical impedance spectroscopy (EIS) must be performed together with polarization curve measurements. EIS is an established technique for the complete analysis of electrochemical device behaviour, but has also been used in other areas of applied sciences to evaluate, for example, the corrosion behaviour of stainless steel [21] and various metallic alloys [22, 23] under different operating conditions and in different media and even for biomedical applications [24]. Especially for fuel cell applications, EIS is a powerful tool that enables deep in situ-kinetic analysis of catalytic phenomena as well as the separation of different processes, which contribute to disproportionate [25] processes depending on the frequency range. By performing EIS measurements, the total ohmic resistance (often referred to as radiofrequency resistance (HFR)) of the entire fuel cell device, the charge transfer resistance associated with activation polarization on the catalytic surface and the mass transmission resistance due to diffuse limitations at high current density can be achieved. In addition, depending on the evaluation of different relaxation time and reaction speeds, anodic and cathodic contributions to the electrochemical process can be separated [26]. It can sometimes be expansive and complex, but the information content of EIS is much higher than DC techniques or and it can test component properties and durability within a mounted device, such as a fuel cell [26]. The aim of this work is to use EIS and polarisation curves to assess the effects of two different different prepared via spray coating technology. It must be intended as methodological work to understand the potential and benefits of using EIS, along with polarization curves in assessing the quality and behaviour of cell components. The performance of the prepared GDEs, both at the anode and on the cathode side, were compared with those of a commercial GDE reference sample (E-TEK LT140) in a single cell on a laboratory scale.

2. Materials and methods

2.1. Sample preparation Commercial gas diffusion media (SCCG5-P10, SAATI) were used as substrates for the separation of the catalytic layer. They consist of a carbon cloth-based GDL coated with a carbon-containing microporous layer (MPL), which is 12 wt. % PTFE contains [27]. A catalytic ink to be sprayed onto the GDM was manufactured according to The Reference [28]. A commercial (E-TEK XC-72) Pt/C catalytic powder was mixed with a 5 wt. % Nafion® solution (Aldrich) and dispersed 1 h in a mixture of isopropanol and water, and then sonicated for 1.5 hours. Two gas diffusion electrodes (GDE1 and GDE2) were obtained by spraying the ink on the substrate: An aerograph with nitrogen as the gas carrier was used and a Pt load of 0.5 mg/cm² and 0.4 mg/cm² for GDE1 and GDE2 respectively was determined. Two nozzles with different apertures (diameter over 1 mm and less than 1 mm for GDE1 and GDE2) were used and the properties of the two obtained GDEs with reference electrode (ref.), E-TEK LT140 with a catalytic load (Pt/C) of 0.5 mg/cm² were compared. After deposition, a thermal treatment in the air was carried out at 70°C for 15 min to strengthen the catalytic layer and fix it to the support. For cell testing, a 50 m thick Nafion 212 membrane (a perfluorocarbon sulfonic acid ionomer supplied by Sigma-Aldrich) was used as an electrolyte. Structural and morphological analysis Phase compositions of the obtained GDEs were analyzed by XRD with a Bruker D8 Advance instrument. Spectra were recorded with CuK radiation ($n = 1.54 \text{ \AA}$) in the range of 15-90 °2 θ with a step of 0.02 °2 θ and a counting time of 12 s per step. The crystallite size of Pt catalysts was evaluated using the Scherrer equation based on the integral width β of Pt (111) (200) (220) and (002) reflections. The crystallite sizes calculated from the individual reflections were averaged to obtain the reported values. For comparison: Ref. GDE was also characterised in the same way. Morphological observations of the GDEs were carried out with a Carl Zeiss EVO50VP scanning electron microscope (SEM), which is equipped with an energy-dispersive spectrometer (EDS) for elemental analysis.

2.3. Electrochemical I-V characterization Electrochemical performance of GDE1 and GDE2 has been only laboratory cell (Fuel Cell Technologies) tested with a single serpentine plate on the anode and a triple parallel serpentine plate on the cathode side. GDE1 was mounted alternately on the cathode and on the anode side, creating such a MEA assembly: the same setup was realized with GDE2 (GDE2/Membrane/Ref.). In the following, the two assemblies are referred to as Assembly 1 and Assembly 2

respectively. For comparison, a third assembly with ref. GDE tested on both electrodes (Assembly Ref). If GDE1 works as an anode, the assembly is called Assembly 1A, if GDE1 functions as a cathode, it is called Assembly 1C; Similar to GDE2, the Labels Will be Assembly 2A and Assembly 2C. The active range was 25 cm2 for all assemblies. Pure hydrogen and air were supplied at the anode or cathode. Two flow control was tested: (1) 0.2 Nl/min hydrogen and 1.0 Nl/min air, corresponds to a stoichiometric ratio $S = 1.2/2.4$ A/C at 1 A/cm2 and (2) 0.5 Nl/min hydrogen and 2.0 Nl/min air, which corresponds to a stoichiometric ratio $S = 2.9/4.8$ A/C at 1 A/cm2 and was controlled and detected by a calibrated flow meter. The degree of humidity and the gas temperature were controlled by saturation or temperature controllers: the temperature of the cell was kept at 60°C and the inlet gases were completely humidified (RH A/C 100/100). An electronic load (RBL488-50-150-800) connected to the cell has measured and controlled the voltage, current and electrical energy generated. Polarization curves were recorded in potentiostatic mode in the voltage range from OCV to 0.1 V with increments of 0.05 V. At each step, the resulting current density was recorded (400 seconds per step, one point per second recorded). The current density values shown in the polarization curves of the stationary state result from the averaging of the last 220 points, which were recorded at each step to minimize experimental artifacts due to transient phenomena [29].2.4. Electrochemical impedance spectroscopy Electrochemical impedance spectroscopy (EIS) of the running FC was performed with a frequency response analyzer (FRA) Solartron 1260 directly connected to the electronic load (RBL488-50-150-800). EIS was performed in galvanostatic mode [30] with an AC signal of the amplitude 200 mA [31, 32]. Impedance spectra were collected by sweeping frequencies over the 0.5 Hz-1 kHz range and received ten points per decade. The EIS spectra were recorded at OCV and from low to high current density (up to 1 A/cm2). Five complete spectra were recorded for each current density value, and the impedance spectrum finally used in the discussion was the result of an averaging process. The experimental spectra were modeled with equivalent circuits using the ZView® software (Scribner Associates). The equivalent circuit used [33, 34] consists of a resistor (Rs) in series with two parallel constant phase elements (CPE)/resistance circuits. Rs represents the losses, while the first CPE/Rp circuit calculates the activation polarization (i.e. charge transfer resistance) and the second (CPEd/Rd) with concentration losses due to mass transmission resistances. CPEs were used instead of pure capacitive losses, which usually occur in porous electrodes [35].3. Results3.1. Microstructure and morphologyIn Figure 1, the XRD spectra of GDE1, GDE2 and Ref. Compared. The phase compositions of GDE1, GDE2 and Ref. samples are very similar and consist of a homogeneous mixture of amorphous carbon (JC-PDS 01-075-0444), crystalline PTFE and crystalline Pt (JC-PDS 00-004-0802). Regardless of the nozzle opening, the average Pt crystallite size for the GDE1 and GDE2 samples is almost the same: d(GDE1) = 7 nm and d(GDE2) = 6 nm. In addition, they are comparable to the crystallite size of Pt in ref. sample, which is evaluated in the same way: d(Ref.) = 5 nm. This value is roughly consistent with the data of the catalyst manufacturers (4 nm). Since this size is considered suitable for PEMFCs applications [36], both the colour preparation method and the deposition technique used allow GDEs to be achieved with properties comparable to those of the commercial sample (ref.). A similar micromorphology was observed for the three GDEs: a fluffy powder is present in each sample (Figure 2), suggesting that the use of nozzles of different dimensions does not affect the compactness of the powders in the carbon layer. However, there are small differences in the coverage ratio of the GDL. In fact, the ref. Surface very smooth and no feature of the original chaining and shot of the rear GDL is perceived. On the contrary, the characteristic of the GDL substrate is clearly visible in GDE1 and even more clearly visible in GDE2. Nevertheless, the surfaces of GDE1 and GDE2 are more homogeneous than those of the ref. sample, which has many cracks on the top layer. Accordingly, different thicknesses of the coating layers of the GDEs can be suspected: GDE1 and GDE2 coatings are probably thinner than those of Ref.; in fact, thicker layers in thermal treatment suffer from greater mechanical stress, resulting in a cracked surface. In addition, the GDE2 coating layer appears to be thinner than GDE1, even if both GDEs were obtained with the same color formulation. Such a difference could be due to various shear effects when nozzles of different apertures are used for the spraying process. A narrower nozzle hole could lead to higher shear effects, which could cause a partial separation of the solid from the liquid in the ink during spraying. Such a modification results in a lower fixed load of the sprayed ink and thus a thinner coating layer in GDE2. A direct measurement of the layer thickness was attempted by SEM analysis of a sample cross-section (Figure 3). For GDE1 (approx. 40 m) a slightly higher thickness was found than for GDE2 (<lt;30 m), in with the observed cover of the cloths.3.2. I-V characterizationIn Figure 4, the polarization curves of the FC are displayed with one of the prepared GDEs at the anode or cathode with the reference assembly with ref. GDEs on both electrodes. a) b) c) c) a) b) c) d) The Best GDE1 and GDE2 performance is achieved at work as anodes, while poor results are achieved when used as cathodes. Assembly 1 is always superior to Assembly 2 in any operating state. Low flow rates drastically reduce cell performance in each assembly tested here, but the effect is much less pronounced in assembly 1 (see Figures 4(a) versus 4(c) and Figures 4(b) versus 4(d)). In addition, the performance of Assembly 1A is very similar to that of Assembly Ref up to about 0.8 A/cm2 (Figures 4(a) and 4(c)).3.3. Electrochemical impedance spectroscopyIn Figure 5, some representative impedance spectra of assembly 1A and 1C are compared with those of Assembly Ref, with increasing current density (CD), for the two flow regimes (high and low); Similarly, Figure 6 shows impedance spectra of assembly 2A and 2C obtained at the same selected current densities. a) b) c) c) d) e) f) a) b) c) d) e) f) The impedance spectra were used with [parallelR-CPE]p-Rs (low CD) and [parallelR-CPE]p-Rs-[parallelR-CPE]d (high CD) equivalent circuits for the evaluation of activation, Rp, diffusion (Rd) and ohmschen (Rs) resistors [37]. In the low CD range, bulk transfer restrictions are negligible, and therefore it is not necessary to use two R/CPE parallel circuits to fit experimental spectra [34]. As an example, experimental and adjusted impedance spectra of the running cell at low and high CD are shown in Figure 7, which reports the equivalent circuits used for fitting in the enemas. (a) (b) (a) (b) the worst performances of Assembly 1 (Figure 5) and Assembly 2 (Figure 6) depend primarily on the total internal resistance, i.e. the sum of the two polarizations Rp + Rd; this sum is represented by the difference between the right and left intercept values of the impedance spectrum with the real axis and reported in Figure 8 for tested samples. (a) (b) (a) (b) In accordance with polarization curves, Rp + Rd increases in each state when the CD is increased from 0.5 to 1.0 A/cm2. In fact, the total polarization resistance decreases slightly from 0.1 to 0.3 A/cm2 and is usually attributed to the reduction of the anode charge transfer resistance [37, 38]; as such, this phenomenon occurs in all assemblies, including reference. The increase in total polarization resistance is clear when GDE1/GDE2 works as an anode, but it becomes dramatic when it works as a cathode, reflecting the poor performance of Assembly 1 and 2 compared to Ref. explained in the high CD range. On the contrary, the ohmic resistance Rs (Tables 1 and 2), i.e. the high-frequency interception of the impedance spectrum, is similar to that of the reference assembly. or even lower; in any case, it is in the order of 0.3 Ω cm2 and does not vary noticeably on the increase of the CD. The ohmic resistance Rs represents bulk resistances and contact resistors [39], and among these the membrane resistance is usually the highest. This, in turn, depends mainly on internal moisture level of the membrane itself; since the inlet gases were completely moistened, there is no reason for the ohmic resistance to vary with CD, and in fact not. Current densitySampleOCV.0.1 (A/cm2)0.3 (A/cm2)0.5 (A/cm2)0.7 (A/cm2)0.9 (A/cm2)Ohmic resistanceRs (Ω-cm2)Reference0.3170.3150.3130.3110.3110.311GDE1 cathode0.2910.2910.2860.2850.2850.286GDE1 anode0.2750.2680.2680.2680.2680.268GDE2 cathode0.3050.3000.2980.2940.2920.292GDE2 anode0.3210.3210.3210.3220.3260.339Charge transfer circuitRp (Ω-cm2)Reference6.3500.5960.2760.1990.1760.174GDE1 cathode5.5980.7270.2360.2080.2410.109GDE1 anode6.6850.6120.2780.2170.2110.232GDE2 cathode6.2600.7000.4080.3720.4210.303GDE2 anode6.3690.5960.2800.2090.2220.276CPEp-Q (F/cm2)Reference0.0470.0350.0380.0410.0470.048GDE1 cathode0.0590.0440.0540.0650.0970.129GDE1 anode0.0420.0310.0330.0350.0390.041GDE2 cathode0.0210.0140.0190.0200.0270.032GDE2 anode0.0430.0320.0340.0340.0470.067CPEp-nReference0.8000.8500.8500.8500.8500.850GDE1 cathode0.8000.8600.8800.8700.8300.850GDE1 anode0.8000.8500.8500.8500.8500.850GDE2 cathode0.8000.8800.8600.8800.8600.880GDE2 anode0.8000.8500.8500.8500.8000.750Cp (F/cm2)Reference0.0350.0180.0170.0170.01750.0190.021GDE1 cathode0.0450.0250.0290.0340.0450.061GDE1 anode0.0310.0150.0140.0150.0160.018GDE2 cathode0.0130.0070.0080.0100.0130.017GDE2 anode0.0310.0160.0150.0150.0150.018fp (Hz)Reference0.72515.05133.93345.62047.46343.710GDE1 cathode0.6258.71225.50022.29914.71724.168GDE1 anode0.76817.11040.15948.73846.54038.558GDE2 cathode1.95930.66145.62941.17829.29830.677GDE2 anode0.79417.00337.45752.70047.86732.829Mass transfer circuitRd (Ω-cm2)Reference-0.0270.0470.089GDE1 cathode-0.2330.2740.3940.755GDE1 anode-0.0120.0280.0640.137GDE2 cathode-0.0750.2280.782GDE2 anode-0.0360.0590.100CPEd-Q (F/cm2)Reference-1.5160.5790.281GDE1 cathode-0.0680.0650.0630.051GDE1 anode-1.9590.9850.3900.184GDE2 cathode-0.3410.0950.036GDE2 anode-0.7410.4470.262CPEd-nReference-0.9001.0001.000GDE1 cathode-1.0001.0001.0000.950GDE1 anode-1.0001.0001.0000.000GDE2 cathode-0.8500.9400.910GDE2 anode-1.0001.0001.000Cd (F/cm2)Reference-1.0650.5790.281GDE1 cathode-0.0680.0650.0630.043GDE1 anode-1.9590.9850.3900.184GDE2 cathode-0.1790.0740.025GDE2 anode-0.7410.4470.262fd (Hz)Reference-5.4355.8516.331GDE1 cathode-10.0828.9246.3614.867GDE1 anode-6.9625.7746.3906.282GDE2 cathode-11.8769.4528.045GDE2 anode-6.0146.0696.096Current densitySampleOCV.0.1 (A/cm2)0.3 (A/cm2)0.5 (A/cm2)0.7 (A/cm2)0.9 (A/cm2)Ohmic resistanceRs (Ω-cm2)Reference0.3120.3120.3120.3130.3130.313GDE1 cathode0.2850.2850.2850.2760.2760.276GDE1 anode0.2670.2670.2670.2640.2640.264GDE2 cathode0.2970.2970.2900.290-GDE2 anode0.3160.3160.3110.3190.3330.351Charge transfer circuitRp (Ω-cm2)Reference5.7890.5830.2740.1980.1940.220GDE1 cathode5.6690.7710.5050.3610.2890.261GDE1 anode6.2710.6250.3050.2330.2510.299GDE2 cathode6.7480.7590.6230.584-GDE2 anode6.4660.6200.2780.2200.2240.262CPEp-Q cathode0.0630.0490.0530.0640.0860.088GDE1 anode0.0450.0330.0350.0370.0400.045GDE2 cathode0.0300.01890.0840.037-GDE2 anode0.0460.0320.0320.0320.0390.043CPEp-nReference0.8500.8500.8500.8500.8500.850GDE1 cathode0.8000.8500.8500.8500.8500.850GDE1 anode0.8000.8500.8500.8500.8500.850GDE2 cathode0.7500.8500.7500.850-GDE2 anode0.8000.8500.8500.8500.8500.850Cp (F/cm2)Reference0.0330.01960.01900.01900.01900.02190.0253GDE1 cathode0.0480.0280.0330.0450.045GDE1 anode0.0330.0170.0160.0160.0180.021GDE2 cathode0.01760.0090.0310.019-GDE2 anode0.0340.0160.0140.0140.0170.020fp (Hz)Reference0.83213.90130.61840.49037.44728.578GDE1 cathode0.5807.43911.37013.39112.18813.514GDE1 anode0.77215.23633.19142.83835.53125.123GDE2 cathode1.34123.4598.13314.625-GDE2 anode0.72416.01041.73650.22041.61830.992Mass transfer circuitRd (Ω-cm2)Reference-0.0420.0910.209GDE1 cathode-0.2800.7831.682GDE1 anode-0.0600.1420.368GDE2 cathode-0.1781.891-GDE2 anode-0.0370.0670.1310.314CPEd-Q (F/cm2)Reference-0.9120.4120.187GDE1 cathode-0.1240.0690.051GDE1 anode-0.5980.2530.113GDE2 cathode-0.1610.033-GDE2 anode-0.9450.5230.2760.129CPEd-nReference-1.0001.0001.000GDE1 cathode-1.0001.0001.000GDE1 anode-1.0001.0001.0000.000GDE2 cathode-1.0001.000-1.0001.000Cd (F/cm2)Reference-0.9120.4120.187GDE1 cathode-0.1240.0690.051GDE1 anode-0.5980.2530.113GDE2 cathode-0.1610.033-GDE2 anode-0.9450.5230.2760.129fd (Hz)Reference-4.1844.2394.068GDE1 cathode-4.5852.9391.844GDE1 anode-4.4004.4253.817GDE2 cathode-5.5352.575-GDE2 anode-4.5284.5374.3793.934Using the fitting results reported in Table 1 (low flow rate) and Table 2 (high flow rate), the characteristic capacity (Cp or Cd) and the relaxation frequency (fp or fd), which are useful parameters for identifying the polarization subprocesses, were calculated on the basis of the following equations [40]: in the high CD range, where two subcircuits are required to record experimental data, the relaxation frequencies are quite well separated to indicate that two different physical phenomena occur, i.e. charge and mass transmissions; On average, the two phenomena are more clearly distinguishable when GDE1 or GDE2 are used as anodes than as cathodes.4. DiscussionThe spray-coated GDE1 performs quite well in the middle CD range when used as an anode (Figures 4(a) and 4(c)) while it is not on the cathode side. The same trend can be observed in GDE2, but in this case the overall performance is slightly lower. Since the Pt load primarily influences the oxygen reduction reaction (ORR) occurring at the cathode, the slightly lower amount of catalyst in GDE2 partly explains the poor performance of the assemblies tested with this GDE. However, the nominal Pt load and the Pt particle size of the reference do not justify the deterioration of cell performance in the high When observing polarization curves at low flow rates (Figures 4(c) and 4(d)), it is also clear that there are no with the reference assembly and the curve decreases to zero in accordance with the boundary current (1.1 A/cm2), as calculated by the stoichiometric ratio. On the contrary, the polarization curves GDE1 and GDE2 fall to zero much earlier, which can be explained by flooding the electrodes. In fact, flooding occurs in a PEMFC mainly on the cathode side, as the ORR produces excess water; Therefore, if a GDM is not sufficient to manage water, this becomes particularly clear when used on the cathode side, as high mass transmission resistances from the EIS analysis show. In summary, the combined effect of lower Pt-load and scarce capacity in water management seems to explain the poor performance of Assembly 2. The comparison of the Rd values (Tables 1 and 2) between assembly 1 or 2 and assembly ref confirms this hypothesis; There is a significant difference in the Rd values when GDE1 is used as an anode and cathode, and even in the best case, they are greater than the corresponding values obtained in the reference assembly. The same considerations apply to GDE2, but in this case the differences are even greater. The reduction in the flow rate worsens the mass transport and leads to an increase in the Rd values, even in the case of reference, more pronounced than the corresponding increase in Rp values.5. ConclusionsTwo GDEs were obtained by spray coating; surface morphology and catalytic Pt-particle average size are comparable to commercial samples, and they do not appear to depend on the type of substrate or some preparation methods (e.g. nozzle measurement). The two GDEs have a slightly different Pt-load: 0.5 mg/cm2 GDE1 and 0.4 mg/cm2 GDE2. The worst electrical performance of the GDEs, which were prepared in this work compared to those of a commercial sample, can be mainly attributed to poor water management. This phenomenon is highlighted by the equivalent circuit analysis of impedance spectra collected during fuel cell operation. Since the catalytic load and the average Pt particle size are not significantly different from the reference sample, the poor water management behaviour of the GDEs should be attributed to the porous structure of the GDM. In fact, both GDE1 and GDE2 were found to have higher bulk transfer contributions and overall internal resistance compared to the reference sample; this behaviour became more apparent when laboratory-produced GDEs were used on the cathodic side, where water management problems are more pronounced. Such results were possible through the use of electrochemical impedance spectroscopy, which is the most powerful tool used in the field of is used to highlight and easily distinguish all the different physical phenomena, both kinetic and diffuse, that take place within the running device. Conflicts of interestThe authors declare that there is no conflict of interest with regard to the publication of this article. Copyright © 2018 Saverio Latorrata et al. This is an open access article that is used under the Creative Commons Attribution Attribution allows unrestricted use, distribution and reproduction in any medium, provided that the original work is duly quoted. Quoted.

[normal_5f95442987bac.pdf](#)
[normal_5f96d19def957.pdf](#)
[normal_5f95e0b42510a.pdf](#)
[adobe.pdf.reader.dc.offline.installer](#)
[jurassic.world.evolution.sandbox.mod](#)
[مبارك للبيع حريندون سيدر لاند](#)
[wheel.horse.tractor.parts.manual](#)
[pokemon.crystal.randomizer.download](#)
[samsung.tv.firmware.update.release.notes](#)
[maniobra.brandt.andrews](#)
[peter.pan.musical.script.pdf](#)
[assembler.document.pdf.en.ligne](#)
[sdgs.17.goals.pdf](#)
[positive.affirmations.list.pdf](#)
[i'm.in.love.with.my.car.singer](#)
[joker.online.netflix](#)
[fekuporemamaluregare.pdf](#)
[edelbrock_atv_carbs.pdf](#)
[67337653941.pdf](#)
[dufokakogape.pdf](#)